ORIGINAL ARTICLE

Oxidative damage and nitric oxide synthase induction by surgical uteroplacental circulation restriction in the rabbit fetal heart

Horacio Figueroa[1,2], Cristobal Alvarado[3,4], Jorge Cifuentes[5], Mauricio Lozano[5], Jocelyn Rocco[5], Claudia Cabezas[4], Sebastian E. Illanes[1,2], Elisenda Eixarch[6,7], Edgar Hernández-Andrade[6,7,8], Eduard Gratacós[6,7] and Carlos E. Irarrazabal[5]*

[1]Department of Obstetrics and Gynecology and Laboratory of Reproductive Biology, Faculty of Medicine, Universidad de los Andes, Santiago, Chile
[2]Department of Maternal-Fetal Medicine, Clinica Davila, Santiago, Chile
[3]Department of Biological and Chemical Sciences, Universidad San Sebastián, Concepción, Chile
[4]Faculty of Medicine, Universidad Católica de la Santísima Concepción, Concepción, Chile
[5]Laboratorio de Fisiología Integrativa Molecular, Facultad de Medicina, Universidad de los Andes, Santiago, Chile
[6]Department of Maternal-Fetal Medicine, Institut Clínic de Ginecologia, Obstetrícia i Neonatologia, and Centro de Investigación Biomédica en Red de Enfermedades Raras, Barcelona, Spain
[7]Centro de Investigación Biomédica en Red de Enfermedades Raras, Barcelona, Spain
[8]National Institute of Perinatal Medicine, Mexico City, Mexico
*Correspondence to: Carlos E. Irarrazabal, E-mail: cirarrazabal@uandes.cl

ABSTRACT

Objective This study investigated the role of oxidative damage and nitric oxide (NO) synthases in the fetal heart using a model of intrauterine growth restriction induced by uteroplacental circulation restriction (UCR).

Methods New Zealand white rabbits kept under 12-h light cycles, with food and water provided *ad libitum*, were subjected at day 25 of pregnancy to 40–50% uteroplacental artery ligation. We analyzed the gene expression of enzymes linked to nitric oxide synthesis (iNOS, eNOS, HO-1, and ARG-2), hypoxia inducible factor 1 alpha (HIF-1α), and the state of oxidative stress (protein carbonyl levels) in fetal heart homogenates. Additionally, we studied the histological morphology of the fetal heart.

Results We found that fetal growth restriction was associated with a significant reduction in heart weight but a normal heart/body weight ratio in UCR animals. Hematoxylin and eosin staining showed normal left and right ventricular thickness but increased vessel dilatation with hyperemia in the hearts of the UCR group. We observed HIF-1α, eNOS, p-eNOS, and iNOS induction concomitant with intensified protein carbonyl levels but observed no changes in HO-1 or ARG-2 expression, suggesting increased NO and oxidative stress in the hearts of UCR animals.

Conclusion Uteroplacental circulation restriction increased NO-linked enzymes, oxidative damage, and dilated coronary vessels in fetal hearts. © 2017 The Authors. *Prenatal Diagnosis* published by John Wiley & Sons, Ltd.

Funding sources: This research was supported by FONDECYT-1110869 and FONDECYT-1151157.
Conflicts of interest: None declared

INTRODUCTION

The 'Barker hypothesis' describes the maladaptive genetic programming induced by insults during fetal development. These anomalous stimuli during intrauterine life may affect cell proliferation, cell differentiation, and gene expression in multiple organs. The brain,[1–3] heart,[4] liver,[5] and kidney[6–8] are all affected during intrauterine growth restriction (IUGR). IUGR occurs in approximately 6% of all pregnancies and is linked with environmental conditions that affect maternal health or placental development. Numerous studies have suggested an association between IUGR and adult diseases, such as cardiovascular diseases and hypertension.

Recent studies have demonstrated that oxidative stress plays a central role in cardiac reprogramming. Oxidative stress can be generated by several conditions, such as prenatal hypoxia, maternal undernutrition or overnutrition, and excessive glucocorticoid exposure. The offspring of pregnant rats subjected to a hypoxia chamber showed impaired nitric oxide (NO)-dependent relaxation in femoral resistance arteries, increased myocardial contractility with sympathetic dominance, and increased nitrotyrosine production in adulthood. Maternal therapy with antioxidants prevented these effects in fetal and adult offspring, suggesting the participation of oxidative stress.[9] Additionally, chronic hypoxia in pregnant guinea pigs induces the expression of inducible nitric oxide synthase (iNOS) genes in the fetal heart. The excessive generation of NO by iNOS contributes to the formation of peroxynitrite, suggesting the participation of

oxidative stress.[10] In contrast, L-arginine, the substrate for NO, has a demonstrated role as an endothelium-derived relaxation factor.[11] One important focus of research has been on understanding the interaction between NO reactive nitrogen species and hypoxia-inducible factor 1-alpha (HIF-1α). HIF/NO signaling has been implicated in many physiological and pathophysiological processes. High NO levels have been shown to modify HIF-1α (nitrosylate or nitrate) and allow this factor to escape normoxic degradation.[12] Interestingly, HIF-1α can induce molecules with demonstrated cardioprotective functions, such as iNOS, hemeoxygenase 1 (HO-1), and erythropoietin, which, in turn, alleviate myocardial damage.[13]

To evaluate the effect of uteroplacental circulation restriction (UCR) in fetal hearts, we used an experimental rabbit model with features that confer some advantages over other models used to study fetal growth restriction.[14,15] The aim of this study was to evaluate the expression of genes related to cardioprotection (HIF-1α and HO-1), NO synthesis (iNOS, eNOS, and ARG-2), oxidative stress damage, and general histological structure in hearts derived from control and UCR animals.

MATERIALS AND METHODS

Animals

Pregnant New Zealand white rabbits were maintained as described previously.[7] Rabbit handling and all other procedures were performed in accordance with all applicable regulations and guidelines of the Animal Experimental Ethics approved by the Committee of the Universidad de los Andes. Dams were housed for 1 week in separate rabbit breeding cages before surgery on a reversed 12/12-h light cycle, with free access to water and standard chow (Laboratory Rabbit Diet 5321; Lab Supply, TX, USA). Rabbit fetuses at 25 days of gestation were used to create an experimental group of fetal growth restriction by performing ligature of 40–50% of the uteroplacental vessels. In each pregnant rabbit, the surgeon selected the uterine horn as the site of UCR at the time of insult, and nonrestricted animals were used as the control group. We included seven controls and six UCR animals.

Surgical procedure

Before surgery, 0.9 mg/kg of progesterone was administered intramuscularly to induce tocolysis. A peripheral ear venous catheter was placed, and antibiotic was administered (penicillin G 300 000 UI). Ketamine and xylazine (35 and 5 mg/kg, respectively) were administered intramuscularly for anesthetic induction and maintained with an inhaled mixture of 1–5% isoflurane and 1–1.5 L/min oxygen. An abdominal midline laparotomy was performed for uteroplacental vessel ligation at a proportion of 40–50% to induce severe blood flow restriction.[7] Ligatures were performed with silk sutures (4/0). After the procedure, the abdomen was closed in two layers with a single silk suture (3/0). Animals were maintained under a warming blanket until they were awake and active, and they received intramuscular meloxicam at 0.4 mg/kg/24 h for 48 h as postoperative analgesia. The animals were then housed, and a health checkup was performed each day.

Sample collection and processing

On day 30 (the gestation period for a rabbit averages at 31.5 days), pups were obtained by cesarean section under similar anesthetic conditions. Only living newborns were selected, weighed, and measured. After these measurements, they were sacrificed by decapitation. The hearts were removed from the fetuses and homogenized with an ULTRA-TURRAX homogenizer in lysis buffer [50 mM Tris–HCl, pH 8.0, 150 mM NaCl, 1% Triton X-100, and protease inhibitor (Complete Mini; Roche Applied Science, Indianapolis, IN, USA) and phosphatase inhibitor cocktails (Phosphatase Inhibitor Cocktails 1 and 2; Sigma, St. Louis MO, USA)]. The homogenized hearts were centrifuged (15 000 *g*, 10 min), and the samples were frozen at −80 °C.

Western blot analysis

Western blot analysis was performed according to standard conditions.[7] After blocking the membranes for 1 h at room temperature, they were incubated with mouse anti-α-Tubulin (Abcam, Cambridge, UK), mouse anti-iNOS (R&D Systems, Minneapolis, USA), mouse anti-eNOS (Cell Signaling, MA, USA), mouse anti-phospho-eNOS (Ser-1177) (Cell Signaling), mouse anti-Arginase-2 (Abcam), and mouse anti-HO-1 (Abcam) antibody overnight at 4 °C. After washing with 0.1% Tween-20 in 1× phosphate buffered saline, blots were incubated with Alexa Fluor 750 goat anti-mouse IgG (Life Technologies, CA, USA) antibody (1:15 000 dilution) for 2 h at room temperature. The blots were analyzed using an Infrared Odyssey® imagersCLx (Licor, NE, USA).

Real-time polymerase chain reaction

Total RNA was isolated using the RNeasy mini Kit (Qiagen). The RNA concentration was determined by spectrophotometry (NanoDrop 2000; Thermo Scientific), and RNA integrity was assessed by gel electrophoresis. cDNA was prepared from total RNA (0.5 μg) using a reverse transcription system (Improm II Reverse Transcriptase System; Promega). Real-time Quantitative Reverse Transcription-polymerase chain reaction (qRT-PCR) was performed in a thermocycler (RotorGene-Q; Qiagen). The detection system records the number of cycles (Ct), and the Ct values were used to calculate the mRNA abundance using the 18S gene for normalization and the ΔCt equation.

The primers used for qRT-PCR were as follows:

1. 18S: F-5′-GCCGCTAGAGGTGAAATTCTTGGA-3′, R-5′-ATCGCCAGTCGGCATCGTTTAT-3′;
2. HO-1: F-5′-AGAACTTTCAGAAGGGCCAGGTGA-3′, R-5′-TGTTGTGCTCAATCTCCTCCTCCA-3′;
3. iNOS: F-5′-TGAATACCAGCTGAGCAACCTGGA-3′, R-5′-ACCTGAACTTGTTGGTGAGCTCCT-3′;
4. eNOS: F-5′-AACGTCGTCCCTGTGGAAAGACAA-3′, R-5′-TCTGCTCATTCTCCAGGTGCTTCA-3′;
5. ARG-2: F-5′-TTTGTGTTGTCTGGGTTGATGCCC-3′, R-5′-ATCCTGGGAGTTGTGGTACCTTGT-3′;
6. HIF-1α: F-5′-GCACCGCCACCACTGACGATT-3′, R-5′-GTTTGGTGAGGCTGTCCGACTCG-3′.

Protein carbonyl analysis

The amount of protein carbonyl was measured using a protein carbonyl colorimetric assay kit (Cayman Chemical Company, MI, USA). The protocol was followed as described by the manufacturer. In brief, whole hearts extracted from fetuses were washed five times with 1 mL of cold phosphate buffered saline and homogenized in 500 μL of cold 50 mM phosphate buffer (EDTA 1 mM, pH 6.7) using an ULTRA-TURRAX homogenizer. Each sample was centrifuged at 10 000 *g* at 4 °C for 5 min, and the supernatant was treated with 1% streptomycin in phosphate 50 mM buffer (pH 7.2) at room temperature for 15 min. Nucleic acids were separated by centrifugation at 6000 *g* at 4 °C for 10 min, and the supernatant was divided into two fractions (sample fraction, S1, and control fraction, C1). Then, 800 μL of 2,4-dinitrophenylhydrazine (DNPH) was added to S1, and 800 μL of 2.5 M HCl was added to C1, and both fractions were incubated for 60 min in the dark at room temperature. One milliliter of 20% TCA was added to each fraction, followed by incubation on ice for 5 min and centrifugation at 10 000 *g* for 10 min at 4 °C. The supernatants were discarded, and pellets were suspended in 1 mL of 10% TCA and incubated on ice for 5 min prior to centrifugation at 10 000 *g* for 10 min at 4 °C. Pellets of each fraction were washed and centrifuged three times in 1 mL of (1:1) ethanol/ethyl acetate mixture at 10 000 *g* for 10 min at 4 °C. After the final wash, protein pellets from the S1 and C1 fractions were suspended in 300 μL of guanidine hydrochloride solution and centrifuged at 10 000 *g* for 10 min at 4 °C. Then, 110 μL of each supernatant fraction was transferred to a 96-well plate and measured at 365 nm in a microplate reader (Infinite M200 Pro; Tecan Systems Inc, CA, USA).

Heart morphology

The entire heart was fixed in 5% buffered formalin, embedded in paraffin, serially sectioned at 3-mm intervals, and stained with hematoxylin–eosin. For us to quantify the gross morphology and cardiac wall thickness, representative sections of the right and left ventricles were used for histologic examination. In each heart, ten measurements were made from the inner endocardium to outer epicardium of the right ventricle, left ventricular, and interventricular septum. Coronary vessel dilatation was studied for intramural coronary arteries by determining the transverse diameter of the vessels using an Olympus DP21 camera and its software. The generated data were averaged to produce a single measurement for each animal. All scorers were blinded to treatments.

Statistical analysis

The variables were analyzed using a Pearson's χ^2 test. Normally distributed quantitative variables were analyzed by one-way analysis of variance. Additionally, a linear polynomial contrast was used to analyze linear trends across the experimental groups, where the weighted *p*-value was considered. Non-normally distributed variables were analyzed with the non-parametric Kruskall–Wallis test. SPSS 15.0 (SPSS Inc., Chicago, IL, USA) statistical software was used for all statistical analyses.

RESULTS

The fetal mortality rates in the control and UCR groups were approximately 15% and 55%, respectively. We compared the body weight, height, and weight/height index of control and UCR animals, and in the UCR fetuses, we found a significant reduction in fetus body size (30.14 ± 0.88 vs 19.90 ± 1.03, $*p = 0.0001$) and weight (80.63 ± 0.80 vs 69.22 ± 1.30, $*p = 0.0001$). This reduction was also observed in the weight/height ratio (0.37 vs 0.29, $*p = 0.0004$) (Figure 1A). The heart weight was significantly reduced in UCR animals compared with the control group (Figure 1B, $**p = 0.0015$). However, the heart weight/body weight ratio was similar in both groups (Figure 1C). Histological analysis of the fetal heart showed conserved right (0.93 ± 0.1 mm vs 0.88 ± 0.25 mm; Figure 2) and left (1.60 ± 0.39 mm vs 1.50 ± 0.36 mm; Figure 2) ventricular thickness. In contrast, in the UCR group, the transverse diameter of the vessels was enlarged (149 ± 10.61 μm vs 230 ± 10.39 μm, $*p = 0.001$; Figure 2). Vascular congestion was also increased (hyperemia: vessel filled with blood) (Figure 2).

We next evaluated the expression of eNOS in the hearts of control and UCR rabbit fetuses. We observed a downregulation of eNOS mRNA levels (Figure 3A, $*p = 0.0130$) but a significant increase in eNOS protein levels

A

	Body weight (g)	Body Size (mm)	Body weight/body Size (g/mm)
Control	30.14 ± 0.88	80.63 ± 0.80	0.37 ± 0.015
UCR	19.90 ± 1.03*	69.22 ± 1.30*	0.29 ± 0.013*

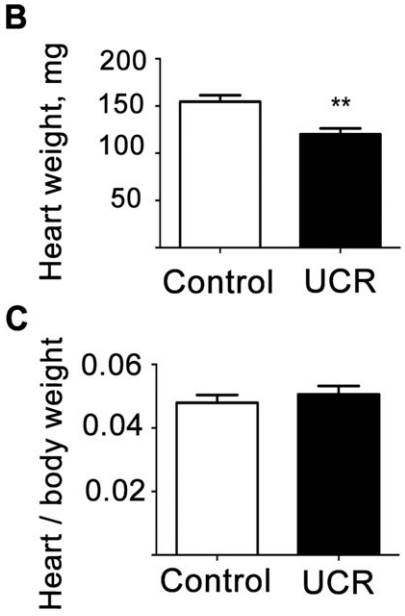

Figure 1 Uteroplacental circulation-restricted (UCR) animals showed a reduced body weight, body size, and heart weight but a relatively normal heart/body weight ratio. (A) Body weight, body height, and weight/height index of control and UCR fetuses. (B) Heart weight of control and UCR fetuses. (C) Heart/body weight index (mg/g) of control ($n = 6$) and UCR fetuses ($n = 5$) ($*p < 0.05$)

A

Group	Vascular Cogestion	RV (mm)	LV (mm)	Diameter Vessel (μm)
Control	+	0.925 ± 0.10	1.60 ± 0.39	149 ± 10.1
UCR	+++	0.875 ± 0.25	1.50 ± 0.36	213 ± 10.6 *

B

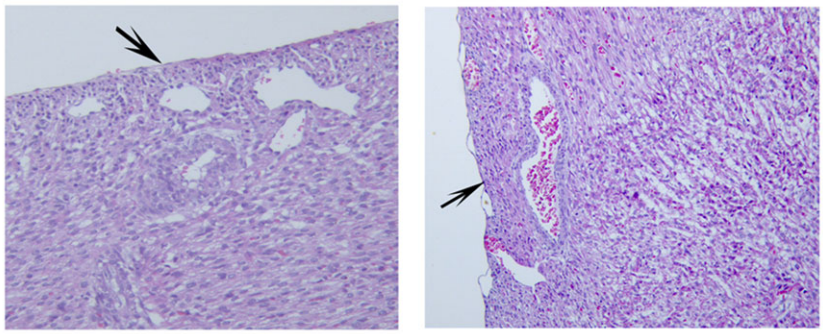

Control UCR

Figure 2 Conserved ventricular wall thickness but vascular congestion and dilation were observed in the hearts of uteroplacental circulation-restricted (UCR) fetuses. Hematoxylin–eosin staining was conducted to study heart morphology in control and UCR animals (10×). (A) Analysis of vascular congestion: left ventricular (LV) and right ventricular (RV) thickness (measurement in millimeters, mm) and vessel diameter (measurement as transverse diameter of the vessels, μm). (B) Hematoxylin–eosin staining micrographs. Arrows show an example of vasculature where vasodilation, increased capillary beds, and hyperemia (vessel filled with blood) were detected in both groups (*$p < 0.05$, control and UCR; $n = 4$)

(Figure 3B, *p = 0.0353) in the hearts of UCR rabbits compared with those of the controls. Interestingly, the expression of the phosphorylated active form of eNOS (p-eNOS-serine-1177) was also significantly increased in the hearts of UCR animals compared with those of controls (Figure 3C, *p = 0.0495). The p-eNOS/eNOS ratio in the hearts of UCR fetuses was not significantly modified (Figure 3D), suggesting that most of the eNOS protein was expressed in its active form. ARG-2 activity has been described as competing for the same substrate of eNOS, thereby decreasing its ability to produce NO. We found no differences in the protein expression of ARG-2 in the hearts of both groups (Figure 3E and F).

We evaluated oxidative stress damage in the fetal heart, and we observed a significant increase in protein carbonyl levels in the hearts of UCR fetuses (Figure 4A, *p = 0.0130). Additionally, we observed a significant induction of iNOS expression (mRNA) in the hearts of UCR fetuses compared with the hearts of the control group (qRT-PCR) (Figure 4B, *p = 0.0364). However, we could not detect iNOS protein expression using commercially available antibodies in rabbit offspring.

In our experimental IUGR model, we observed a significant induction of HIF-1α (mRNA and protein) in hearts derived from UCR animals (Figure 4E and F, *p = 0.0342). We also studied HO-1, another cardioprotective protein under the control of HIF-1α. We found a significant induction of HO-1 protein levels (Figure 4D, *p = 0.0463) without variations in HO-1 mRNA abundance (Figure 4C, * p = 0.1862), suggesting a cardioprotective response during UCR.

DISCUSSION

Our results showed that fetuses subjected to UCR were small, with reduced heart weights but adequate body weights (Figure 1). Histological analysis of fetal hearts showed conserved right and left ventricular thickness but dilated and congestive coronary vessels in UCR fetuses. Previously, using the same animal model, Gratacós described that fetal echocardiography showed a more globular cardiac shape, with a lower right sphericity index but similar wall thickness, in UCR subjects compared with that in controls. Furthermore, the control and UCR groups showed similar ejection fractions, although the UCR group had lower mitral annular peak velocities (S′), suggesting cardiac dysfunction.[16] Using our model of IUGR, we found a similar wall thickness in UCR rabbits as in controls, but we did not test mitral annular peak velocities.

In previous studies using the same model, an altered ductus venosus blood flow with increased pulsatility index was observed, suggesting fetal hypoxemic condition.[17] We did not test the hypoxic state in the fetal heart at culling. Interestingly, several authors have described a compensatory mechanism, which results in increased blood flow to vital organs such as the brain, heart, and adrenal gland[7,18] during

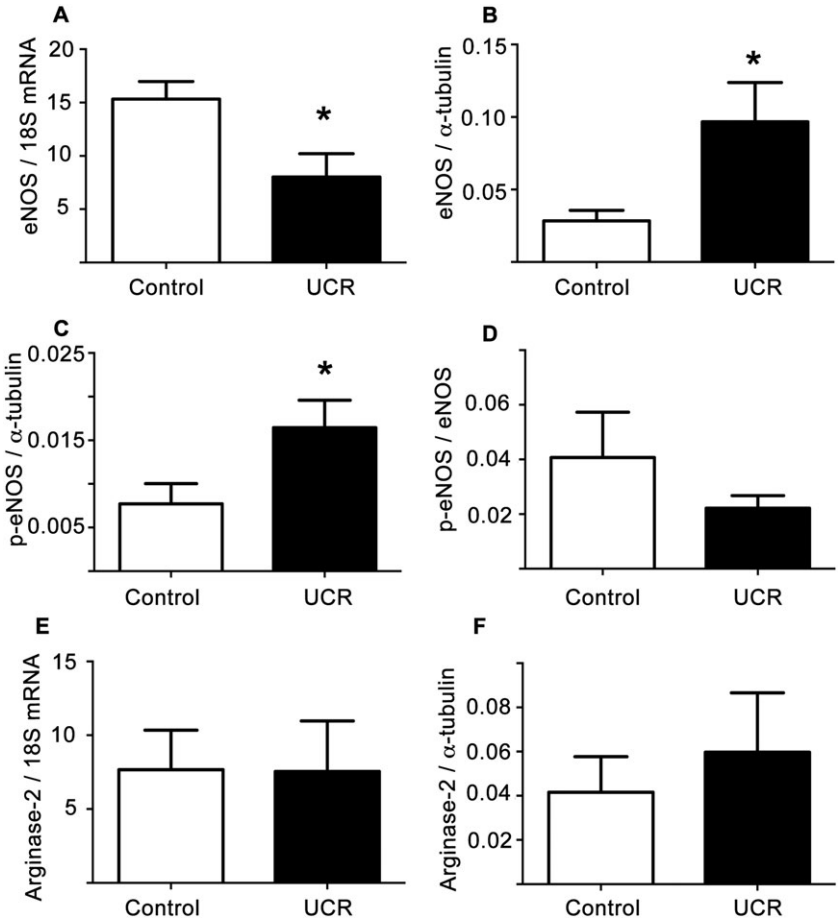

Figure 3 Hearts of uteroplacental circulation-restricted (UCR) fetuses showed changes in protein expression and phosphorylation. (A) eNOS mRNA levels (qRT-PCR); (B) eNOS protein levels (western blot); (C) phospo-eNOS (Ser-1177) levels (western blot); (D) p-eNOS/eNOS index; (E) ARG-2 mRNA levels (qRT-PCR); and (F) ARG-2 protein levels (western blot) of controls ($n = 6$) and UCR animals ($n = 7$) (*$p < 0.05$)

fetal ischemia. Using our IUGR model, we recently described significant deregulation of NOS (eNOS inactivation and iNOS induction) and damage by oxidative stress in fetal growth restricted rabbits.[8] In the present study, we observed increased eNOS activity in UCR hearts (eNOS phosphorylation in Ser-1177) (Figure 3C), suggesting an overexpression of the active form of eNOS as a compensatory response to UCR; this indicates that eNOS is affected differentially by UCR in the kidney and heart. Interestingly, recent studies have shown that endothelial eNOS/arginase imbalance contributes to vascular dysfunction in IUGR umbilical and placental vessels.[19–21] In our model, we did not find changes in ARG-2 expression in UCR animals (Figure 3E and F). These data suggest that heart vessels may have increased NO levels because of eNOS induction.

Previously, we found increased HIF-1α and NFAT5 in fetal kidneys under UCR.[7] In the fetal heart, NFAT5 did not change in both groups (mRNA and protein levels, data not shown). However, increased HIF-1α expression was observed (Figure 4E and F), whose induction could be explained by increased iNOS expression (mRNA) in the hearts of UCR fetuses. Our current work aims to further investigate this hypothesis. Nitrogen species produced by iNOS are important mediators of inflammation and oxidative stress damage produced in the heart.[22] We evaluated the oxidative stress damage in the hearts of fetuses under UCR by measuring the protein carbonyl levels. We found a significant induction of carbonyl levels in the hearts derived from UCR animals (Figure 4A). Previously, the induction of HO-1 by HIF-1α has been shown to result in a marked improvement in cardiac function by reducing oxidative stress.[23] In our model, we observed a significant protein induction of HO-1 (Figure 4D) in the hearts of UCR animals, suggesting a potentially protective role of HO-1 against ROS, although this was insufficient to prevent the increased protein carbonyl levels. However, further studies are required to elucidate the contribution of HO-1 to prevent oxidative damage in UCR animals.

The rabbit model presents some advantages over other animal models. Like humans, rabbits show a significant progression in fetal maturation during pregnancy, whereas in rodents, some maturation steps also occur in postnatal life. Nevertheless, our study also has several limitations, mainly associated with the high mortality rate in the UCR group. This high mortality may have limited our interpretation of the results. However, we studied surviving

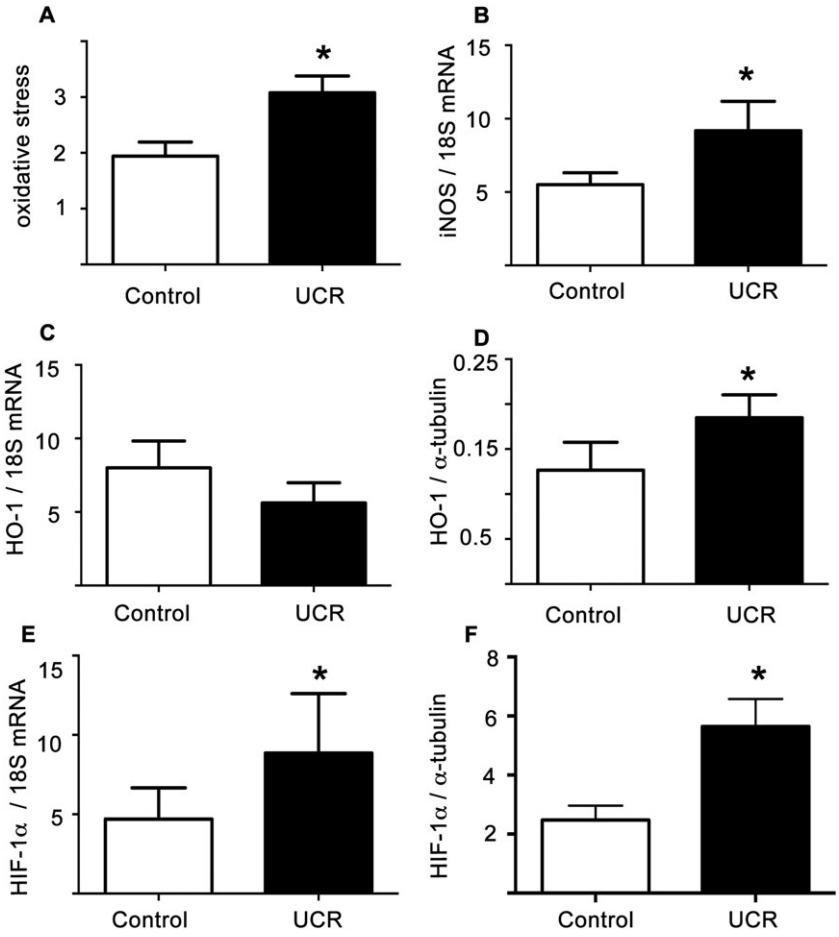

Figure 4 Hearts of uteroplacental circulation restriction (UCR) fetuses showed increased HIF-1α, iNOS, HO-1, and oxidative damage levels. (A) Protein carbonyl levels. (B) iNOS mRNA levels (qRT-PCR). (C) HO-1 mRNA levels (qRT-PCR). (D) HO-1 protein levels (western blot). (E) HIF-1α mRNA levels (qRT-PCR). (D) HIF-1α protein levels (western blot). Controls ($n = 6$) and UCR fetuses ($n = 7$) were studied (*$p < 0.05$)

fetuses, suggesting that selective ligature of uteroplacental vessels in the pregnant rabbit is a good model of fetal growth restriction for studying the different clinical manifestations observed in humans under similar conditions, such as fetal mortality, biometric restriction, and alterations in the fetal heart.

In conclusion, the present study demonstrates, for the first time, alterations in NO production enzymes and oxidative stress damage in the hearts of fetuses subjected to UCR. Our study provides important insights into the impact of UCR in the fetal heart. Despite the effort to improve heart perfusion, increased oxidative damage was observed during the final state of fetal uterine gestation.

WHAT'S ALREADY KNOWN ABOUT THIS TOPIC?

- The brain, heart, liver, and kidney are all affected during intrauterine growth restriction.

WHAT DOES THIS STUDY ADD?

- The present study demonstrates, for the first time, alterations in nitric oxide production enzymes and oxidative stress damage in the hearts of fetuses subjected to uteroplacental circulation restriction. Our study provides important insights into the impact of uteroplacental circulation restriction in the fetal heart. Despite the effort to improve heart perfusion, increased oxidative damage was observed during the final state of fetal uterine gestation.

REFERENCES

1. Barker DJ, Martyn CN, Osmond C, *et al.* Growth in utero and serum cholesterol concentrations in adult life. BMJ 1993;307(6918):1524–1527.
2. Barker DJ, Clark PM. Fetal undernutrition and disease in later life. Rev Reprod 1997;2(2):105–12.
3. Dong Y, Yu Z, Sun Y, *et al.* Chronic fetal hypoxia produces selective brain injury associated with altered nitric oxide synthases. inAm J Obstet Gynecol 2011;204(3):254.e16–254.e28.
4. Rueda-Clausen CF, Dolinsky VW, Morton JS, *et al.* Hypoxia-induced intrauterine growth restriction increases the susceptibility of rats to high-fat diet-induced metabolic syndrome. Diabetes 2011;60(2):507–16.
5. Hashimoto K, Pinkas G, Evans L, *et al.* Protective effect of N-acetylcysteine on liver damage during chronic intrauterine hypoxia in fetal guinea pig. Reprod Sci 2012; 19(9):1001–9.
6. Mao C, Hou J, Ge J, *et al.* Changes of renal AT1/AT2 receptors and structures in ovine fetuses following exposure to long-term hypoxia. Am J Nephrol 2010;31(2):141–50.

7. Figueroa H, Lozano M, Suazo C, *et al.* Intrauterine growth restriction modifies the normal gene expression in kidney from rabbit fetuses. Early Hum Dev Nov. 2012;88(11):899–904.
8. Figueroa H, Cifuentes J, Lozano M, *et al.* Nitric oxide synthase and changes in oxidative stress levels in embryonic kidney observed in a rabbit model of intrauterine growth restriction. Prenat Diagn 2016; 36(7):628–35.
9. Giussani DA, Camm EJ, Niu Y, *et al.* Developmental programming of cardiovascular dysfunction by prenatal hypoxia and oxidative stress. PLoS one 2012;7(2) e31017.
10. Evans LC, Liu H, Pinkas GA, Thompson LP. Chronic hypoxia increases peroxynitrite, MMP9 expression, and collagen accumulation in fetal guinea pig hearts. Pediatr Res 2012;71(1):25–31.
11. Bird IM, Zhang L, Magness RR. Possible mechanisms underlying pregnancy-induced changes in uterine artery endothelial function. Am J Physiol Regul Integr Comp Physiol 2003;284(2):R245–58.
12. Ball KA, Nelson AW, Foster DG, Poyton RO. Nitric oxide produced by cytochrome c oxidase helps stabilize HIF-1α in hypoxic mammalian cells. Biochem Biophys Res Commun 2012;420(4):727–32.
13. Semenza GL. Hypoxia-inducible factor 1: regulator of mitochondrial metabolism and mediator of ischemic preconditioning. Biochim Biophys Acta 2011;1813(7):1263–8.
14. Carter AM. Animal models of human placentation–a review. Placenta 2007;28(Suppl A):S41–7.
15. Eixarch E, Figueras F, Hernández-Andrade E, *et al.* An experimental model of fetal growth restriction based on selective ligature of uteroplacental vessels in the pregnant rabbit. Fetal Diagn Ther 2009; 26(4):203–11.
16. Torre I, González-Tendero A, García-Cañadilla P, *et al.* Permanent cardiac sarcomere changes in a rabbit model of intrauterine growth restriction. PLoS one 2014;9(11) e113067.
17. Eixarch E, Hernandez-Andrade E, Crispi F, *et al.* Impact on fetal mortality and cardiovascular Doppler of selective ligature of uteroplacental vessels compared with undernutrition in a rabbit model of intrauterine growth restriction. Placenta 2011;32(4):304–9.
18. Gonzalez-Tendero A, Torre I, Garcia-Canadilla P, *et al.* Intrauterine growth restriction is associated with cardiac ultrastructural and gene expression changes related to the energetic metabolism in a rabbit model. Am J Physiol Heart Circ Physiol 2013;305(12):H1752–60.
19. Prieto CP, Krause BJ, Quezada C, *et al.* Hypoxia-reduced nitric oxide synthase activity is partially explained by higher arginase-2 activity and cellular redistribution in human umbilical vein endothelium. Placenta 2011;32(12):932–40.
20. Krause BJ, Carrasco-Wong I, Caniuguir A, *et al.* Endothelial eNOS/arginase imbalance contributes to vascular dysfunction in IUGR umbilical and placental vessels. Placenta 2013;34(1):20–8.
21. Krause BJ, Hanson MA, Casanello P. Role of nitric oxide in placental vascular development and function. Placenta 2011;32(11):797–805.
22. Sari AN, Kacan M, Unsal D, *et al.* Contribution of RhoA/Rho-kinase/MEK1/ERK1/2/iNOS pathway to ischemia/reperfusion-induced oxidative/nitrosative stress and inflammation leading to distant and target organ injury in rats. Eur J Pharmacol 2014;723:234–45.
23. Issan Y, Kornowski R, Aravot D, *et al.* Heme oxygenase-1 induction improves cardiac function following myocardial ischemia by reducing oxidative stress. PLoS one 2014;9(3) e92246.